Parton Degrees of Freedom: Connected and Disconnected Sea Partons from CT18 Parametrization of PDFs

Tie-Jiun Hou
Northeastern University, China

Work with Jian Liang(UKY), Keh-Fei Liu(UKY), Meng-Shi Yan(PKU) and C.-P. Yuan(MSU)

May 15, 2021
微扰量子场论研讨会, 上海

CT18CS Global PDF Analysis

An alternative parametrization of CT18 for $\bar{u}$ and $\bar{d}$ at $Q_0 = 1.3$ GeV scale with an input from Lattice QCD.

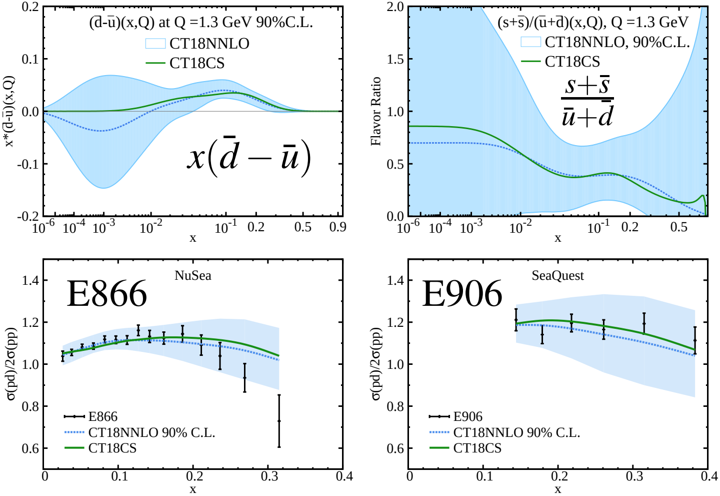

Brief Review of Global PDF Analysis

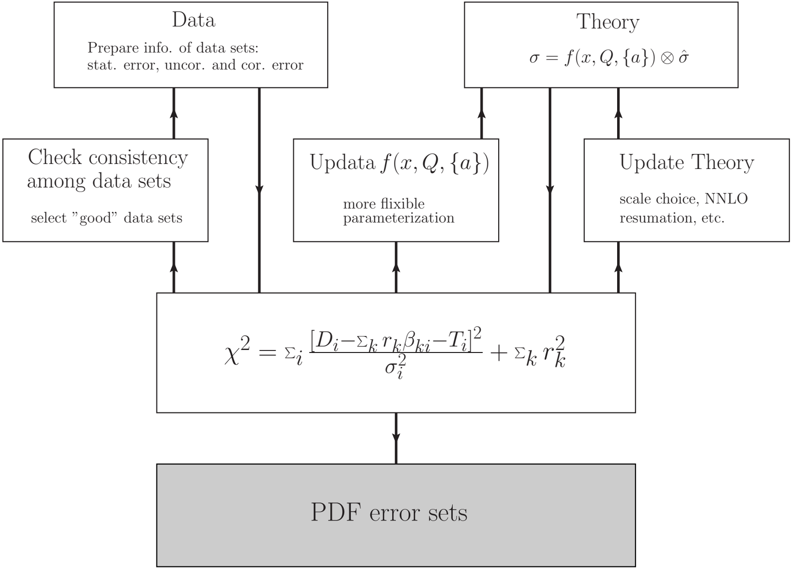

LHC data sets included in CT18

245	1505.07024	LHCb Z (W) muon rapidity at 7 TeV
246	1503.00963	LHCb 8 TeV Z rapidity
249	1603.01803	CMS W lepton asymmetry at 8 TeV
250	1511.08039	LHCb Z (W) muon rapidity at 8 TeV
253	1512.02192	ATLAS 7 TeV Z p_T
542	1406.0324	CMS incl. jet at 7 TeV with R=0.7
544	1410.8857	ATLAS incl. jet at 7 TeV with R=0.6
545	1609.05331	CMS incl. jet at 8 TeV with R=0.7
573	1703.01630	CMS 8 TeV $t\bar{t}$ (p_T, y_t) double diff. distributions
580	1511.04716	ATLAS 8 TeV $t\bar{t}$ p_T and $m_{t\bar{t}}$ diff. distributions
248	1612.03016	ATLAS 7 TeV Z and W rapidity $\rightarrow$ CT18Z PDFs

(PRD, arXiv: 1912.10053, T.- J. Hou *et al.*)

Theory calculations @NNLO

Obs.	Expt.	fast table	NLO code	K-factors	R,F scales
Inclusive jet	ATL 7 CMS 7/8	APPLgrid fastNLO	NLOJet++	NNLOJet	p_T, p_T^1
p_T^Z	ATL 8	APPLgrid	MCFM	NNLOJet	$\sqrt{Q^2 + p_{T,Z}^2}$
W/Z rapidity W asymmetry	LHCb 7/8 ATL 7 CMS 8	APPLgrid	MCFM/aMCfast	FEWZ/MCFM	$M_{W,Z}$
DY (low,high mass)	ATL 7/8 CMS 8	APPLgrid	MCFM/aMCfast	FEWZ/MCFM	Q_{ll}
$t\bar{t}$	ATL 8 CMS 8	fastNNLO			$\frac{H_T}{4}, \frac{m_T}{2}$

- For Drell-Yan data and jet data, NNLO prediction are down by using NLO prediction from applgrid/fastNLO times NNLO/NLO K-factor.
- For $t\bar{t}$ data, NNLO prediction are down by using NNLO prediction from fastNLO directly.

  the MC integration of NNLO cross sections.

Non-perturbative forms of PDFs in CT18 at $Q_0 = 1.3\text{GeV}$

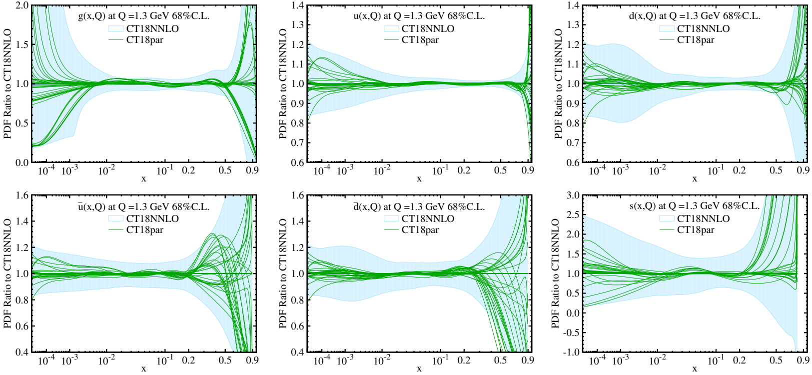

- CT18 – sample result of exploring various non-perturbative parametrization forms at $Q_0 = 1.3$ GeV.
- There is no data to constrain very large and very small x region.

Non-perturbative forms of PDFs in CT18 at $Q_0 = 1.3$ GeV

In CT18, 6 d.o.f of partons are parametrized at $Q_0 = m_c = 1.3$ GeV $\gg \Lambda_{QCD}$,

$$g, \quad u^v, \quad d^v, \quad \bar{u}, \quad \bar{d}, \quad s.$$

Where $\bar{s}(x) \equiv s(x)$ is assumed, and $u = u^v + \bar{u}$ and $d = d^v + \bar{d}$.
Heavier parton, like c, b and t, are generated through PDF evolution.
The functional form for the 6 parton flavors is

$$f^i(x, Q = Q_0) = a_0^i x^{a_1^i - 1}(1-x)^{a_2^i} P^i(x)$$

- $x \to 0$: $f^i \propto x^{a_1^i - 1}$, Regge-like behavior
- $x \to 1$: $f^i \propto (1-x)^{a_2^i}$, quark counting rules
- $P^i(x; a_3, a_4, \ldots)$: affects intermediate x. In CT18, Bernstein polynomial is applied.

Requirements for PDF parametrization

- Valence quark number sum rule

$$\int_0^1 [u(x) - \bar{u}(x)]dx = 2, \quad \int_0^1 [d(x) - \bar{d}(x)]dx = 1$$

$$\int_0^1 [s(x) - \bar{s}(x)]dx = 0$$

- Momentum sum rule

$$\sum_{a=q,\bar{q},g} \int_0^1 x f_{a/p}(x,Q)dx = 1$$

In total, there are 29 shape parameters used in CT18.
As a result, the full CT18 global fit yields $\chi^2 = 4292$, with a total of 3681 data points, and $\chi^2/N_{pt} = 1.17$.

Gottfried sum rule

Gottfried sum rule (1967) was originally obtain by assuming $\bar{u}$ and $\bar{d}$ to be the same, which leads to

$$S_G = \int_0^1 \frac{dx}{x}\left[F_2^p(x) - F_2^n(x)\right] = \frac{1}{3}, \quad \text{with } \bar{d}(x) \equiv \bar{u}(x)$$

New Muon Collaboration (NMC – PRL 66, 2712 (1991), PRD 50, R1 (1994)), $\mu + p(n) \to \mu + X$, obtained

$$S_G = 0.235 \pm 0.026 \quad (\ Q = 2\text{GeV}\ )$$

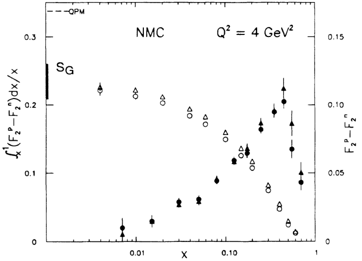

Gottfried sum rule

The correct expression of sum rule is,

$$S_G = \frac{1}{3} - \frac{2}{3}\int_0^1 dx\left(\bar{d}(x) - \bar{u}(x)\right) + O(\alpha_s^2).$$

Hence, NMC data gives

$$\int_0^1 dx\left(\bar{d}(x) - \bar{u}(x)\right) = 0.147 \pm 0.039, \quad \text{at } Q = 2 \text{ GeV}$$

The following experiments like HERMES (PLB387, 419 (1996)) and E866 (PRD64, 052002 (2001)) also shown preference of $\bar{u}/\bar{d}$ flavor asymmetry.

Experiment	$\langle Q^2 \rangle$ (GeV^2)	$\int_0^1 [\bar{d}(x) - \bar{u}(x)]dx$
NMC/DIS	4.0	0.147 ± 0.039
HERMES/SIDIS	2.3	0.16 ± 0.03
FNAL E866/DY	54.0	0.118 ± 0.012

What is the origin of $\int dx \left(\bar{d}(x) - \bar{u}(x)\right) \neq 0$?

Hadronic tensor in Euclidean path-integral formalism

Motivated by Hadronic tensor in QCD path-integral formalism in Euclidian space.

u^{v+cs} $\qquad$ $\bar{u}^{cs}$ $\qquad$ $u^{ds},\ \bar{u}^{ds}$

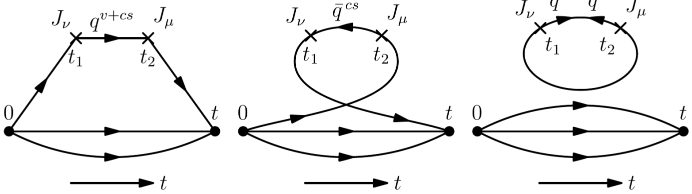

Connected sea(CS) Disconnected sea(DS)

$$
\begin{aligned}
u &= u^{v+cs} + u^{ds}, \quad & d &= d^{v+cs} + d^{ds} \\
\bar{u} &= \bar{u}^{cs} + \bar{u}^{ds}, \quad & \bar{d} &= \bar{d}^{cs} + \bar{d}^{ds}
\end{aligned}
$$

Define $u^v \equiv u^{v+cs} - \bar{u}^{cs}$, which is equivalent to defining $u^{cs} \equiv \bar{u}^{cs}$.

Hence,

$$
\begin{aligned}
u - \bar{u} &\equiv (u^{v+cs} + u^{ds}) - (\bar{u}^{cs} + \bar{u}^{ds}) = u^v + (u^{ds} - \bar{u}^{ds}) \\
&\neq u^v, \quad \text{unless } u^{ds} = \bar{u}^{ds}
\end{aligned}
$$

Similarly, $d^v \equiv d^{v+cs} - \bar{d}^{cs}$.

Hadronic tensor in Euclidean path-integral formalism versus Quasi-PDF from Lattice QCD

- Path-Integral Formalism

q^{v+cs}, $\bar{q}^{cs}$ $\quad$ $\bar{q}^{cs}$ $\quad$ q^{ds}, $\bar{q}^{ds}$

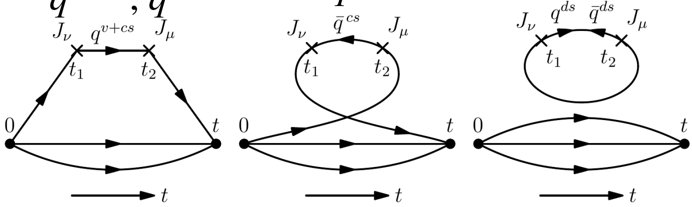

- Quasi-PDF from Lattice QCD

q^{v+cs}, $\bar{q}^{cs}$ $\quad$ q^{ds}, $\bar{q}^{ds}$

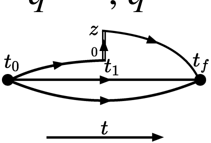

Connected Insertion(CI)

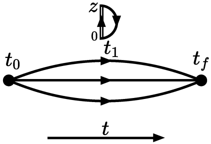

Disconnected Insertion(DI)

Quasi PDF results from LP3 and ETMC - connected insertion calculation

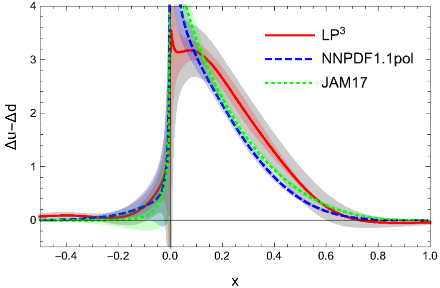

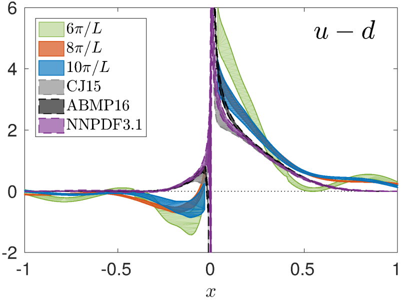

LP3 – H.W. Lin et al, PRL, arXiv:1807.07431

C. Alexandrou et al, PRL, arXiv:1803.02685

Where

$$q(x > 0) = q^{v+cs}(x), \qquad q(x < 0) = -\bar{q}^{cs}$$

Parton degrees of freedom are the same as in hadronic tensor - K.F. Liu, PRD, arXiv:2007.15075

Lattice input to global fitting of PDFs

Lattice result from overlap on $N_f = 2+1$ DWF on 4 lattices, with one at physical pion mass (J. Liang et al., χQCD,PRD,arXiv:1901.07526)

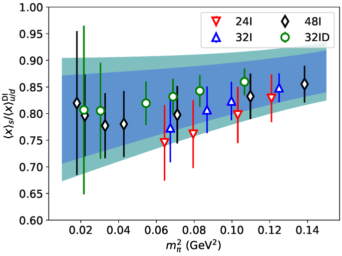

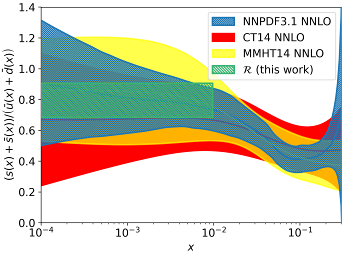

$$\frac{1}{R} = \frac{\langle x \rangle_{s+\bar{s}}}{\langle x \rangle_{\bar{u}+\bar{d}}(DI)}(\text{at } 1.3 \text{ GeV}) = 0.822(69)(78)$$

This is the only Lattice data used in the CT18CS analysis.

Strategy for global analysis in CT18CS

In CT18CS, the non-perturbative PDFs parametrized at $Q_0 = 1.3$ GeV are :

$$g, \quad u^v, \quad d^v, \quad \bar{u}^{cs}, \quad \bar{d}^{cs}, \quad s^{ds}.$$

In this analysis,

- Disconnected Sea (DS) components:
  - Similar to CT18 fit, we assume $\bar{s}(x) = s(x)$. Hence, $s^{ds}(x) = \bar{s}^{ds}(x)$.
  - Likewise, we also assume $u^{ds}(x) = \bar{u}^{ds}(x)$ and $d^{ds}(x) = \bar{d}^{ds}(x)$ for simplicity.
  - Assuming isospin symmetry for u and d quark PDF

  This leads to

$$u^{ds} = \bar{u}^{ds} = d^{ds} = \bar{d}^{ds} = Rs = R\bar{s},$$

With $1/R = 0.822$ at $Q_0 = 1.3$ GeV.

Parton degrees of freedom at $Q_0 = 1.3$ GeV

- Connected Sea (CS) components:
  We define $u^{cs} \equiv \bar{u}^{cs}$ and $d^{cs} \equiv \bar{d}^{cs}$. They will be separately determined by the global fit, though with the same a_1 and a_2 components.

The physical parton degrees of freedom used in CT18CS are then:

In CT18

$$\begin{aligned} g &= g_{par} \\ u^v &= u^v_{par} \\ d^v &= d^v_{par} \\ \bar{u} &= \bar{u}^{cs} + \bar{u}^{ds} = \bar{u}_{par} + Rs_{par} \\ \bar{d} &= \bar{d}^{cs} + \bar{d}^{ds} = \bar{d}_{par} + Rs_{par} \\ s &= \bar{s} = s_{par} \end{aligned}$$

In CT18CS

Both CT18 and CT18CS have 6 independent non-perturbative PDF functions, hence 6 parton degrees of freedom, at Q_0 scale.
The PDFs $f(x,Q)$ at $Q > Q_0$ are obtained by applying DGLAP evolution equations, as in CT18.

Global Analysis - CT18

The global analysis of CT18 has already included the data of NMC and E866, and thus reflect the $\bar{u} \neq \bar{d}$.

ID#	Experimental data set		N_{pt}	χ^2	χ^2/N_{pt}	S_E
160	HERAI+II 1 fb^{-1}, H1 and ZEUS NC and CC $e^{\pm}p$ reduced cross sec. comb.	[27]	1120	1408(1378)	1.3(1.2)	5.7(5.1)
101	BCDMS F_2^p	[65]	337	374 (384)	1.1(1.1)	1.4(1.8)
102	BCDMS F_2^d	[66]	250	280 (287)	1.1(1.1)	1.3(1.6)
104	NMC F_2^d/F_2^p ← NMC	[67]	123	126 (116)	1.0(0.9)	0.2(-0.4)
108†	CDHSW F_2^p	[68]	85	85.6 (86.8)	1.0(1.0)	0.1(0.2)
109†	CDHSW F_3^p	[68]	96	86.5 (85.6)	0.9(0.9)	-0.7(-0.7)
110	CCFR F_2^p	[69]	69	78.8(76.0)	1.1(1.1)	0.9(0.6)
111	CCFR xF_3^p	[70]	86	33.8(31.4)	0.4(0.4)	-5.2(-5.6)
124	NuTeV $\nu\mu\mu$ SIDIS	[71]	38	18.5(30.3)	0.5(0.8)	-2.7(-0.9)
125	NuTeV $\bar{\nu}\mu\mu$ SIDIS	[71]	33	38.5(56.7)	1.2(1.7)	0.7(2.5)
126	CCFR $\nu\mu\mu$ SIDIS	[72]	40	29.9(35.0)	0.7(0.9)	-1.1(-0.5)
127	CCFR $\bar{\nu}\mu\mu$ SIDIS	[72]	38	19.8(18.7)	0.5(0.5)	-2.5(-2.7)
145	H1 σ_r^b	[73]	10	6.8(7.0)	0.7(0.7)	-0.6(-0.6)
147	Combined HERA charm production	[74]	47	58.3(56.4)	1.2(1.2)	1.1(1.0)
169	H1 F_L	[30]	9	17.0(15.4)	1.9(1.7)	1.7(1.4)
201	E605 Drell-Yan process	[75]	119	103.4(102.4)	0.9(0.9)	-1.0(-1.1)
203	E866 Drell-Yan process $\sigma_{pd}/(2\sigma_{pp})$ ← E866	[76]	15	16.1(17.9)	1.1(1.2)	0.3(0.6)
204	E866 Drell-Yan process $Q^3 d^2\sigma_{pp}/(dQdx_F)$	[77]	184	244 (240)	1.3(1.3)	2.9(2.7)
225	CDF Run-1 electron A_{ch}, $p_{T\ell} > 25$ GeV	[78]	11	9.0(9.3)	0.8(0.8)	-0.3(-0.2)
227	CDF Run-2 electron A_{ch}, $p_{T\ell} > 25$ GeV	[79]	11	13.5(13.4)	1.2(1.2)	0.6(0.6)
234	DØ Run-2 muon A_{ch}, $p_{T\ell} > 20$ GeV	[80]	9	9.1(9.0)	1.0(1.0)	0.2(0.1)
260	DØ Run-2 Z rapidity	[81]	28	16.9(18.7)	0.6(0.7)	-1.7(-1.3)
261	CDF Run-2 Z rapidity	[82]	29	48.7(61.1)	1.7(2.1)	2.2(3.3)
266	CMS 7 TeV 4.7 fb^{-1}, muon A_{ch}, $p_{T\ell} > 35$ GeV	[83]	11	7.9(12.2)	0.7(1.1)	-0.6(0.4)
267	CMS 7 TeV 840 pb^{-1}, electron A_{ch}, $p_{T\ell} > 35$ GeV	[84]	11	11.8(16.1)	1.1(1.5)	0.3(1.1)
268†‡	ATLAS 7 TeV 35 pb^{-1} W/Z cross sec., A_{ch}	[85]	41	44.4 (50.6)	1.1(1.2)	0.4(1.1)
281	DØ Run-2 9.7 fb^{-1} electron A_{ch}, $p_{T\ell} > 25$ GeV	[86]	13	22.8(20.5)	1.8(1.6)	1.7(1.4)
504	CDF Run-2 inclusive jet production	[87]	72	122 (117)	1.7(1.6)	3.5(3.2)
514	DØ Run-2 inclusive jet production	[88]	110	113.8 (115.2)	1.0(1.0)	0.3(0.4)

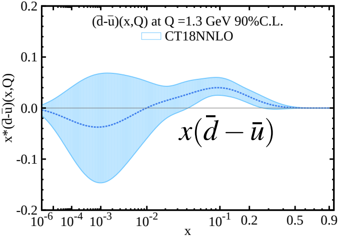

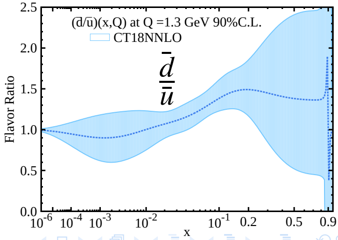

E906/SeaQuest

$$\frac{\sigma(pd)}{2\sigma(pp)}$$

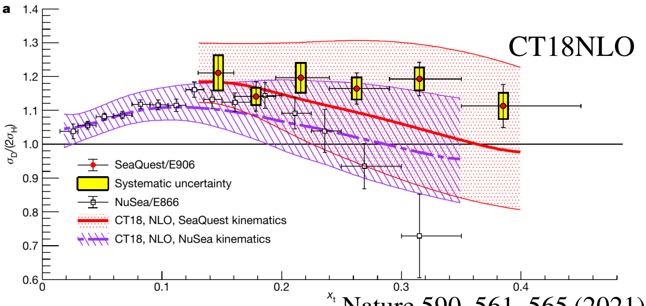

Nature 590, 561–565 (2021), Dove, J. *et al*

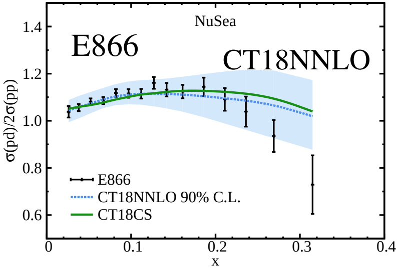

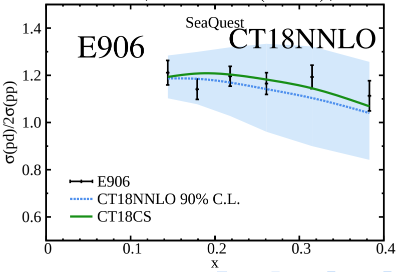

Small-x behavior of CT18CS PDFs

The non-perturbative PDF functions are chosen so that

- $\bar{d}/\bar{u} \xrightarrow{x\to 0} 1.$ $\Leftarrow$ Isospin symmetry, similar to CT18
- $\bar{u}^{ds}, \bar{d}^{ds}, \bar{s}^{ds} \xrightarrow{x\to 0} x^{-1}.$ $\Leftarrow$ Similar to CT18

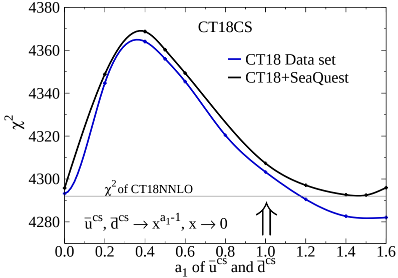

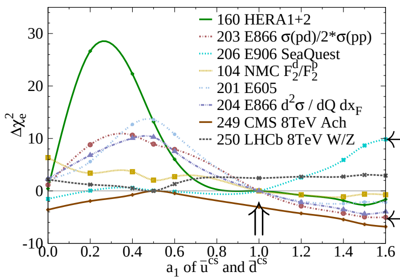

$\longleftarrow$ E906

$\longleftarrow$ E866

- We scan the a_1 parameter of $\bar{u}^{cs}$ and $\bar{d}^{cs}$, and choose $a_1 = 1.0$ as CT18CS, where most of data are well fitted.
- The SeaQuest data was not included in the global fit.
- CT18CS has total $\chi^2 = 4299$ for $N_{pt} = 3681$. CT18 has total $\chi^2 = 4292$, only lower by 7 units.

CT18CS PDFs

With the input of $\bar{u}^{ds} = \bar{d}^{ds} = Rs^{ds}$ from lattice QCD, and considering the scenario of small-x behavior, we obtain the CT18CS at $Q_0 = 1.3$ GeV scale.

$$\frac{1}{R} \equiv \frac{\langle x \rangle_{s+\bar{s}}}{\langle x \rangle_{\bar{u}+\bar{d}}(DI)}$$

$$= 0.822$$

at 1.3 GeV

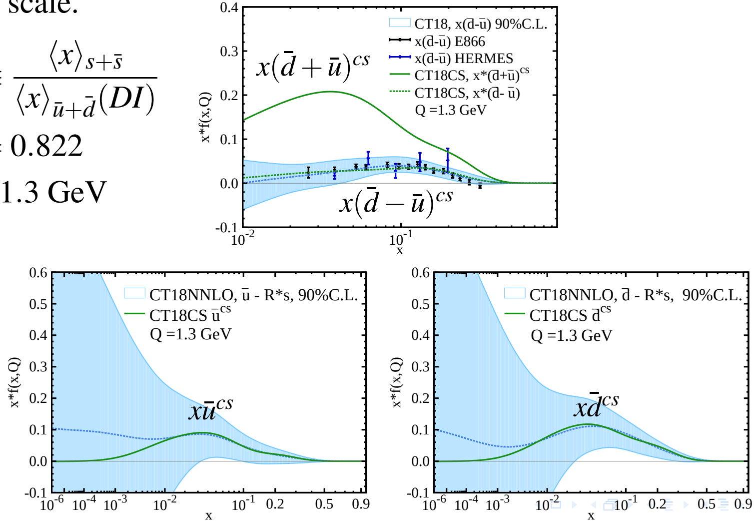

CT18CS PDFs

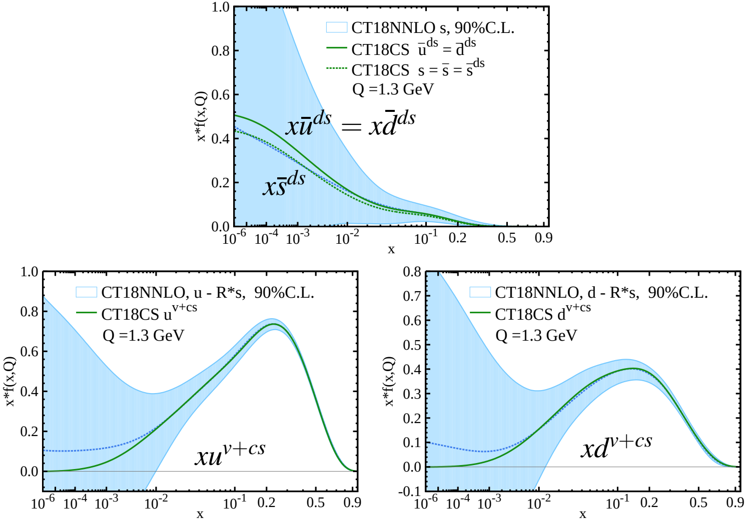
CT18NNLO s, 90%C.L.
CT18CS ū^ds = d̄^ds
CT18CS s = s̄ = s̄^ds
Q =1.3 GeV
$x\bar{u}^{ds} = x\bar{d}^{ds}$
$x\bar{s}^{ds}$
x*f(x,Q)
x
CT18NNLO, u - R*s, 90%C.L.
CT18CS u^v+cs
Q =1.3 GeV
xu^{v+cs}
CT18NNLO, d - R*s, 90%C.L.
CT18CS d^v+cs
Q =1.3 GeV
xd^{v+cs}

CT18CS PDFs

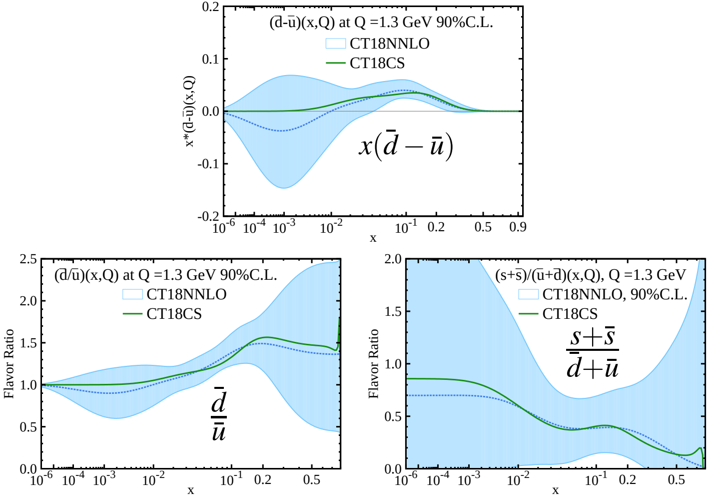

(d̄-ū)(x,Q) at Q =1.3 GeV 90%C.L.
CT18NNLO
CT18CS
$x(\bar{d}-\bar{u})$
x*(d̄-ū)(x,Q)
x
(d̄/ū)(x,Q) at Q =1.3 GeV 90%C.L.
CT18NNLO
CT18CS
$\frac{\bar{d}}{\bar{u}}$
Flavor Ratio
(s+s̄)/(ū+d̄)(x,Q), Q =1.3 GeV
CT18NNLO, 90%C.L.
CT18CS
$\frac{s+\bar{s}}{\bar{d}+\bar{u}}$

The $\langle x \rangle$ Moment of CT18CS at 1.3 GeV

The $\langle x \rangle$ moment of CT18CS at 1.3 GeV:

u^{v+cs}	d^{v+cs}	$\bar{u}^{cs}$	$\bar{d}^{cs}$	$2u^{ds}(2d^{ds})$	$2s^{ds}$	gluon
0.335	0.157	0.013	0.021	0.038	0.026	0.386

More direct comparison between global analysis and lattice calculation can be done one by one, instead of being limited to $u - d$ and s.

	$\mu = 2.0$ GeV		$\mu = 1.3$ GeV
	CT18	Lattice	CT18CS
$\langle x \rangle_{u^+ - d^+}$	0.156(7)	0.184(32)	0.172
$\langle x \rangle_{s^+}$	0.033(9)	0.092(41)	0.026

$$u^+ - d^+ = (u + \bar{u}) - (d + \bar{d}) = (u^{v+cs} + u^{ds} + \bar{u}^{cs} + \bar{u}^{ds}) - (d^{v+cs} + d^{ds} + \bar{d}^{cs} + \bar{d}^{ds})$$

$$\xrightarrow{CT18CS} (u^{v+cs} - d^{v+cs}) + (\bar{u}^{cs} - \bar{d}^{cs})$$

$$s^+ = s + \bar{s} = s^{ds} + \bar{s}^{ds} \xrightarrow{CT18CS} 2s^{ds}$$

Allow direct comparison between lattice calculations and global analysis for each parton degree of freedom.

Summary

- With the input from lattice QCD, $\frac{1}{R} \equiv \frac{\langle x \rangle_{s+\bar{s}}}{\langle x \rangle_{\bar{u}+\bar{d}}(DI)}$, we consider global analysis with the connected sea parton degrees of freedom taken into account, which are respondsible for $\bar{u} \neq \bar{d}$, as suggested by data.

- The result of global analysis, the CT18CS, is found to be compatible with CT18.

- The CT18CS allows to provide direct comparison between lattice calculations and global analysis for each parton degree of freedom.

Hadronic tensor in Euclidean path-integral formalism

- DIS in Minkowski space $\frac{d^2\sigma}{dE'd\omega} = \frac{\alpha^2}{q^4}\frac{E'}{E} l^{\mu\nu} W_{\mu\nu}$

$$W_{\mu\nu}(\vec{q},\vec{p},\nu) = \frac{1}{\pi}\mathrm{Im}T_{\mu\nu} = \langle N(\vec{p})| \int \frac{d^4x}{4\pi} e^{iq\cdot x} J_\mu(x) J_\nu(0) |N(\vec{p})\rangle_{spin\ ave.}$$
$$= \frac{1}{2}\sum_n \int \prod_{i=1}^{n}\left[\frac{d^3p_i}{(2\pi)^3 2E_{pi}}\right](2\pi)^3\delta^4(p_n - p - q)\langle N(\vec{p})|J_\mu(0)|n\rangle\langle n|J_\nu(0)|N(\vec{p})\rangle_{spin\ ave.}$$

- Euclidean path-integral

(K.F. Liu and S.J. Dong, PRL 72, 1790 (1994), K.F. Liu, PRD 62, 074501 (2000))

$$\widetilde{W}_{\mu\nu}(\vec{q},\vec{p},\tau)$$
$$= \frac{1}{4\pi}\sum_n \frac{2m_N}{E_n}\delta(\vec{p}_n - \vec{p} - \vec{q}) < N(\vec{p})|J_\mu|n >< n|J_\nu|N(\vec{p}) >_{spin\ ave.} e^{-(E_n - E_p)\tau}$$
$$= < N(\vec{p})|\sum_{\vec{x}} \frac{e^{-i\vec{q}\cdot\vec{x}}}{4\pi} J_\mu(\vec{x},\tau) J_\nu(0,0)|N(\vec{p}) >_{spin\ ave.}$$

Inverse problem
(Laplace transform)

$$D(\tau) = \int K(\tau,\nu)\rho(\nu)d\nu,$$
$$D(\tau) = \widetilde{W}_{\mu\nu}(\tau), \quad K(\tau,\nu) = e^{-\nu\tau}, \quad \rho(\nu) = W_{\mu\nu}(q^2,\nu)$$

PDF on Lattice: Quasi-PDF

Problem: No light-cone direction on Euclidean lattice.

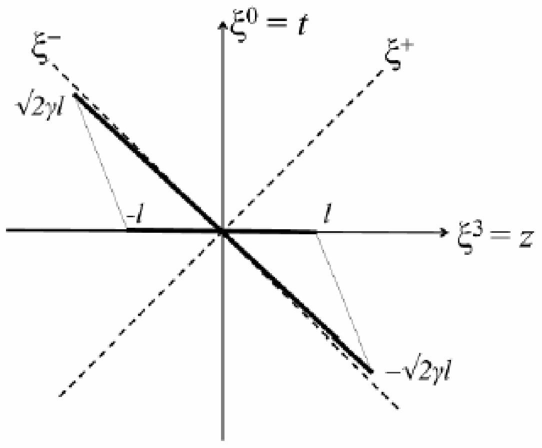

Credit: *Ji,PRL.2013*

Alternative approach:
spatial separation
↓ *boost*
light-like separation

Quasi-PDF:

Can be calculated on lattice

$$\tilde{q}(x, \mu_R, P^z) = \int \frac{dz}{4\pi} e^{-ix\cdot zP^z} \langle N|\bar{\psi}(z)\Gamma W(z,0)\psi(0)|N\rangle$$

Large Momentum Effective Theory (LaMET) [Ji,PRL.2013]:

$$\tilde{q}(x, \mu_R, P_z) = \int_{-1}^{1} \frac{dy}{|y|} C(\frac{x}{y}, \frac{\mu_R}{\mu}, \frac{\mu}{yP^z}) q(y, \mu) + O\left(\frac{\Lambda^2_{\rm QCD}}{P_z^2}, \frac{m_N^2}{P_z^2}\right)$$

Strange quark and antiquark Quasi-PDFs

- Not a valence quark of the nucleon.
- Only disconnected contribution $\langle N|\bar{\psi}(z)\Gamma W(z,0)\psi(0)|N\rangle$ on Lattice.

Disconnected insertion diagrams are more difficult to calculate on Lattice. The first attempt was done in arXiv: 2005.01124 (by Rui Zhang, Huey-Wen Lin and Boram Yoon)

$$\mathrm{Re}[h(z)] \propto \int dx\,(s(x) - \bar{s}(x))\cos(xzP_z)$$

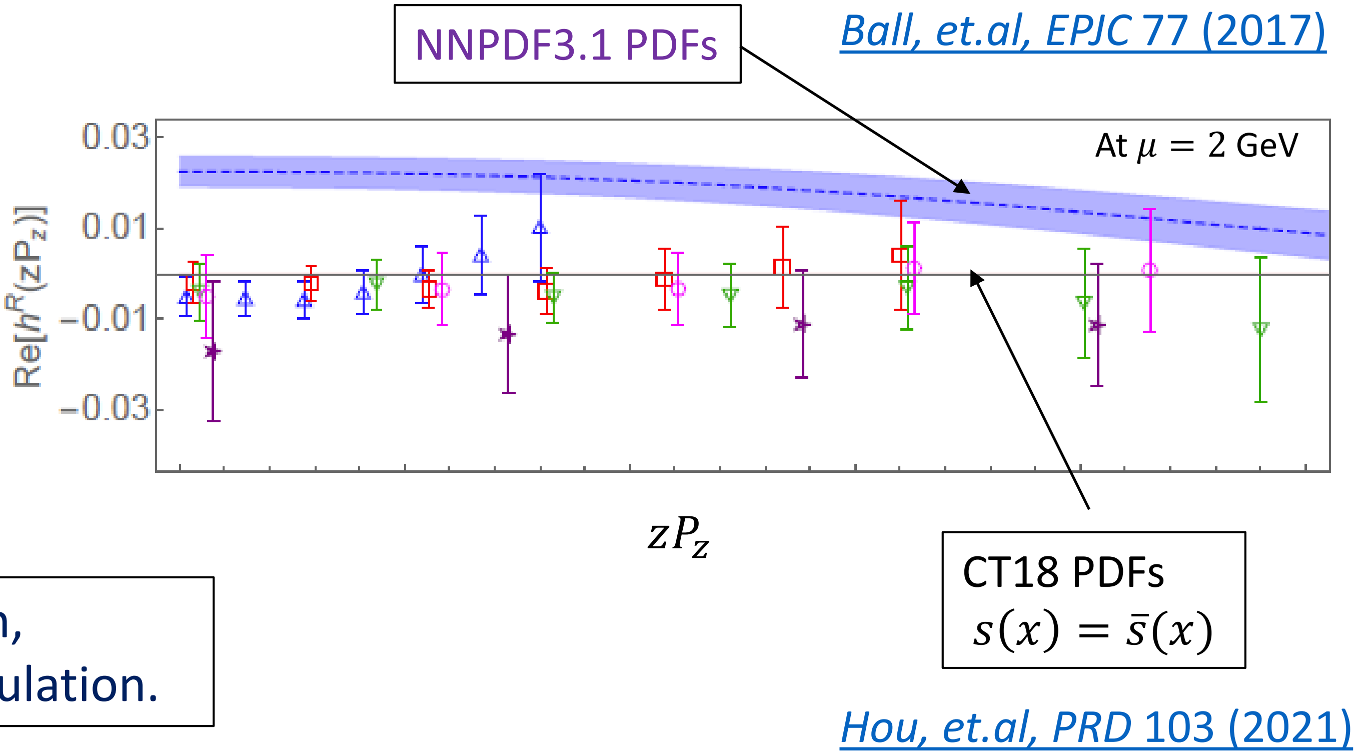

$s(x) = \bar{s}(x)$ is a good approximation, to be consistent with Quasi-PDF calculation.